Plant Science 362 (2026) 112846

Contents lists available at ScienceDirect

Plant Science

journal homepage: www.elsevier.com/locate/plantsci

Genome-wide identification of the *CIPK* family in sunflower (*Helianthus annuus* L.) and functional analysis of HaCIPK18 in salt tolerance

Chenchang Wang [a,1], Qixiu Huang [b,1], Jiafeng Gu [a], Maohong Cai [a], Zhonghua Lei [b], Liang Liang [a,*], Tao Chen [a,*]

[a] School of Life and Environmental Science, Hangzhou Normal University, Hangzhou 311121, China
[b] Institute of Crop research, Xinjiang Academy of Agricultural Sciences, Urumqi, China

ARTICLE INFO

Keywords:
Helianthus annuus
CIPK family
HaCIPK18
Salt tolerance
CBL-CIPK signaling

ABSTRACT

Soil salinization poses a serious threat to global agriculture, driving the need to uncover the genetic basis of crop salt tolerance. Although the CBL-interacting protein kinase (CIPK) family is a known mediator of plant stress responses, its specific functions in the sunflower (*Helianthus annuus* L.), a salt-tolerant crop, remain poorly defined. Here, we identified 36 *CIPK* genes in the sunflower genome. Comparative analysis with the CIPK families of *Arabidopsis thaliana*, rice (*Oryza sativa*), and lettuce (*Lactuca sativa*) revealed evolutionarily conserved relationships and structural features. Under salt stress, RNA sequencing and qRT-PCR analyses demonstrated a significant upregulation of *HaCIPK18* in both root and leaf tissues. To dissect the functional role of HaCIPK18, we silenced *HaCIPK18* in sunflower using virus-induced gene silencing (VIGS). Salt-treated *HaCIPK18*-silenced plants exhibited severe leaf damage, elevated reactive oxygen species (ROS) accumulation, and reduced biomass compared to controls, directly linking HaCIPK18 to salt tolerance. Notably, *HaCIPK18* showed elevated expression in reproductive tissues, which may imply dual roles in stress adaptation and development. Our study not only provides the first comprehensive overview of the *CIPK* family in sunflower but also pinpoints HaCIPK18 as a promising candidate for breeding crops resilient to saline soils.

1. Introduction

Abiotic stressors have a major impact on plant growth. Large areas of agricultural land are now affected by these stresses, leading to a marked reduction in agricultural yields(Kopecká et al., 2023). Abiotic stressors such as high salinity, heat and cold trigger complex signaling mechanisms (Kollist et al., 2019), which highlights why it matters for plants to fine-tune their cellular responses for optimal adaptation. Among these stressors, salinity is especially detrimental. Due to drier soils, excessive salinity is predicted to affect 6 % of all arable land and 20 % of irrigated fields(Yang & Guo, 2018). Projections suggest that by 2050, drought and salinity could result in soil salinization that impacts more than 50 % of arable land(Chen et al., 2021b). Thus, it is crucial to investigate the self-protection mechanisms that plants use in response to saline–alkaline stress.

Calcium ions (Ca^{2+}) act as versatile second messengers, triggering calcium-dependent signal transduction pathways in plants(Patra et al., 2021, Wang et al., 2024). The key players in these processes are Ca^{2+} sensors, which include calmodulin (CAMs), calmodulin-like proteins (CMLs), calmodulin-dependent protein kinases (CDPKs) and calcineurin B-like proteins (CBLs)(Kudla et al., 2010, Hashimoto & Kudla, 2011). CBLs act primarily as calcium signal receivers, lacking the enzymatic capacity to transmit signals downstream (Luan et al., 2002). Instead, they interact with CBL-interacting protein kinases (CIPKs), forming the CBL-CIPK signaling pathway that mediates plant responses to abiotic stress(Ma et al., 2020, Kaya et al., 2024).

CIPKs are Ser/Thr protein kinases named for their interaction with CBLs. They serve as intermediaries in the CBL-mediated calcium signaling cascade, facilitating downstream calcium signal transmission (Kour et al., 2023). These kinases are essential for plant adaptation to environmental stresses(Khan et al., 2023). CIPKs typically possess a serine/threonine kinase domain at the N-terminus, a regulatory domain at the C-terminus, and a variable linker domain between them (Albrecht et al., 2001). The C-terminal domain contains a conserved NAF/FLSL

* Corresponding authors.
E-mail addresses: liangliang@hznu.edu.cn (L. Liang), chentao@hznu.edu.cn (T. Chen).
[1] indicates co-first authors

https://doi.org/10.1016/j.plantsci.2025.112846
Received 6 August 2025; Received in revised form 5 October 2025; Accepted 26 October 2025
Available online 31 October 2025

motif, which is crucial for CIPK binding to CBLs (Mao et al., 2016). Upon sensing calcium signals, CBLs bind to the NAF/FLSL motif at the CIPK C-terminus; this interaction induces conformational changes in the C-terminal regulatory domain—changes that relieve autoinhibition of the N-terminal kinase domain and thereby activate the phosphorylation activity of CIPKs(Gong et al., 2004, Zhang et al., 2023). Following this activation, CIPKs modulate calcium signal pathways by phosphorylating specific serine/threonine residues in downstream target proteins(Zhang et al., 2023).

CIPKs have been studied across various species. In *Arabidopsis thaliana*, CIPK24 binds to CBL4(Liu et al., 2000) and phosphorylates SOS1 (salt overly sensitive 1) to expel excess Na^+ from cells (Yin et al., 2020). Similarly, CBL10 in *Arabidopsis* phosphorylates *NHX* (Na^+/H^+ antiporter), which facilitates vacuolar sequestration of excess cytosolic Na^+ upon salt stress-induced calcium signaling, thereby maintaining cytoplasmic ion homeostasis.(Kim et al., 2007). In a similar vein, *GbCIPK6* in cotton (*Gossypium hirsutum* L.) under salt stress interacts with *CBL* to activate the Na^+/H^+ reverse transporter protein, *GbNHX7*, which facilitates sodium compartmentalisation to alleviate ion toxicity (Akram et al., 2020). *OsCIPK9*, a member of the *CIPK* family in rice, has also been shown to negatively regulate the expression of this gene by interacting with OsSOS3, leading to reduced tolerance to salt stress in rice (Zhou et al., 2023). In addition to the above genes, ectopic expression of the *OsCIPK17-OsCBL2/3* module, which is involved in salt response in rice, in *Arabidopsis* was able to enhance the ability of aboveground parts in transgenic *Arabidopsis* to exclude Na^+, thereby increasing the salt tolerance of the plants(Qin et al., 2024).

Additionally, under low potassium conditions, *Arabidopsis AtCIPK9/23* dynamically regulates potassium ion uptake and remobilisation by phosphorylating *AtCBL1/9/2/3*(Li et al., 2023). In oilseed rape, a link between six *BnaCBLs* and 17 *BnaCIPKs* has now been identified, and the pathways involved in salt signaling have been further defined(Zhang et al., 2014). And after overexpression of *Arabidopsis CIPK* family member *AtCIPK16* in wheat, the growth phenotype of overexpressed wheat under salt stress was significantly better than that of the control group, which proved that it could improve the tolerance of wheat to salt stress(Imtiaz et al., 2023). Maize *CIPK* family members *ZmCIPK21* and *ZmCIPK42* have also been shown to play a role in the salt-responsive pathway, with heterologous overexpression of *ZmCIPK21* decreasing intracellular Na^+ accumulation in *Arabidopsis thaliana* subjected to salt stress, whereas overexpression of *ZmCIPK42* resulted in enhanced tolerance to high salinity in both maize and *Arabidopsis*(Chen et al., 2021a).

Sunflower (*Helianthus annuus* L.), a globally significant oilseed crop with substantial economic value(Smith, 2014).exhibits remarkable tolerance to saline-alkaline stress(Shi & Sheng, 2005). This adaptive capacity has established the species as a model system for investigating plant responses to abiotic stressors (Moroldo et al., 2024). However, the genome-wide identification and functional characterization of CIPK genes in sunflower remains underexplored.

In this study, we identified 36 members of the sunflower *CIPK* gene family using the sunflower whole genome. Subsequent integrated bioinformatics analyses enabled comprehensive characterization of their physicochemical properties, phylogenetic relationships, and gene structures. Expression analysis of RNA-seq data from the Sunflower Transcriptome Universal Database revealed that *HaCIPK18* was upregulated under salt stress. Additionally, functional validation through virus-induced gene silencing (VIGS) of *HaCIPK18* revealed its critical role in salt tolerance regulation.

2. Materials and methods

2.1. Identification and annotation of CIPKs homologs in Helianthus annuus L

Genome sequences of sunflower (*H. annuus*) were downloaded from the Ensembl Plants database (https://plants.ensembl.org/, accessed on 20 March 2024). After downloading the sequences of the 26 known *Arabidopsis* CIPK gene family members from TAIR, they were used as a query to search the Sunflower Protein Database (https://blast.ncbi.nlm.nih.gov/Blast.cgi?PROGRAM=blastp&PAGE_TYPE=BlastSearch&LINK_LOC=blasthome, accessed on 20 March 2024) using BLASTP with the e value set to 1×10^{-5}. Meanwhile, based on the structural domain analysis of CIPK proteins, resulting in the download of HMM models of Pkinase (PF 00069) and NAF (PF 03822) from the Pfam database (http://pfam.xfam.org/, accessed on 22 March 2024). The protein database was searched using the TBtools-II with an E-value threshold of 0.01. Next, the detection results of the two methods were compared and the common sequence ID was selected. Ip (isoelectric point) and MW (molecular weight) analysis were performed using the online website (http://web.expasy. org/protparam/, accessed on 13 July 2024) and subcellular localization prediction was accomplished by https://wolfpsort.hgc.jp/, accessed on 14 July 2024. The amino acid sequences and nucleic acid sequences of *HaCIPKs* are in Supplementary File S1.

2.2. Physicochemical characterization and subcellular localization prediction of CIPKs in Helianthus annuus L

Ip (isoelectric point) and MW (molecular weight) analysis were performed using the online website (http://web.expasy.org/protparam/, accessed on 13 July 2024) and subcellular localization prediction was accomplished by https://wolfpsort.hgc.jp/, accessed on 14 July 2024. The amino acid sequences and nucleic acid sequences of *HaCIPKs* are in Supplementary File S1.

2.3. Phylogenetic tree analysis of CIPK proteins

To get a deep insight into the evolutionary expansion of the sunflower CIPK gene family, the peptide sequences of CIPKs from *H. annuus*, *Arabidopsis thaliana*, *Oryza sativa* and *Lactuca sativa*. were used to reconstruct the phylogeny of *CIPK* gene family. The phylogenetic analysis of the CIPK gene family was done by using the Neighbor-Joining (NJ) method as implemented in MEGA software, which was estimated using the JTT model.

2.4. Chromosomal location density and gene collinearity analysis of CIPK genes in Helianthus annuus L

Based on gene annotation information, the bioinformatics software TBtools (V2.080) was used to analyze the chromosomal location and density of sunflower *CIPK* family genes. The requisite data for this investigation were downloaded from the Ensembl Plants database. Pairwise all-against-all BLAST analysis was performed for sunflower and other plant species protein sequences. The results generated from this BLAST analysis, along with the GFF3 annotation files, were then determined by the Multiple Collinearity Scan toolkit (MCScanX, V2.3.1) to discern syntenic relationships and potential collinear gene arrangements within the analyzed genomes.

2.5. Conserved domains and gene structure analysis of CIPK genes in Helianthus annuus L

The Conserved Domain Database (CDD) from NCBI (/https://www.ncbi.nlm.nih.gov/cdd/, accessed on 5 June 2024) was used to generate functional domain diagrams. The MEME Suite 5.5.7 (https://meme-suite.org/, accessed on 6 June 2024) was used for the prediction of conserved motifs. Concurrently, the obtained conserved motifs were visualised using the Gene Structure View program in TBtools, resulting in the generation of a gene structure map.

2.6. Cis-regulatory elements analysis in CIPK promoters

The promoter sequences of the sunflower CIPK family gene was obtained by PlantCARE (https://bioinformatics.psb.ugent.be/webtools/plantcare/html/, accessed on 10 June 2024) and visualised using the Simple Biosequence Viewer (V2.080) program in TBtools.

2.7. Plant growth conditions and treatments

The plant material employed was the AZB variety of sunflower. Two layers of paper were moistened with sterile water and placed together to form paper beds. Sunflower seeds were placed between the paper beds and the beds were transferred into Petri dishes and incubated under a photoperiod of 16 h of light and 8 h of darkness for three days. During this period, the temperature was maintained at 25°C to encourage seed germination. Following germination, 10 uniformly germinated seedlings per biological replicate were transferred to hydroponic containers containing a 1/5 Hoagland's nutrient solution for further incubation, with 3 containers per group. After a two-week growth period, the seedlings were exposed to a salt stress treatment, during which 200 mM NaCl was introduced into the hydroponic containers. The leaves from the samples treated with NaCl were collected at 3-hour intervals, specifically at 3, 6, and 9 h post-treatment. Untreated plants' leaves were used as controls. All 10 seedlings within a single hydroponic container were combined to collect leaves, thereby minimizing tissue heterogeneity. In total, three biological replicates were collected. The collected leaves were immediately frozen in liquid nitrogen and stored at −80°C for later RNA extraction. RNA was extracted from each leaf sample for subsequent analysis using qRT-PCR.

2.8. RNA extraction, cDNA synthesis, and quantitative real-time PCR

Total RNA was isolated from the aforementioned plant material using the Trizol reagent. In addition, the gDNA Clean Reaction Mix Ver.2 (Accurate Biology, Hunan, China) was utilised for the removal of gDNA, and the EvoM-MLVRT Reaction Mix Ver.2 was employed for the reverse transcription. A total of 1 μg of total RNA was synthesised into cDNA. Subsequently, qRT-PCR assays were performed using a CFX 96 Touch Real-Time PCR Detection System (Bio-Rad, Hercules, CA, USA) in a 10 μL reaction volume. The qRT-PCR primary mixture used was ChamQ universal SYBR qPCR Master Mix (Vazyme, Nanjing, China). Three biological replicates were used to extract RNA from sunflowers, and these experiments were repeated independently three times. *HaTubulin* was used as a reference gene. The primers used for qPCR are listed in Table S2.

2.9. Construction of TRV-VIGS-based vectors

The TRV-based vector system comprises two components RNA1 and RNA2, and the binary VIGS vectors pTRV1and pTRV2 have been described in.

The TRV-RNA2 vector was digested with EcoRI and BamHI restriction enzymes (Thermo Scientific), Gene fragments were cloned with Phanta UC Super-Fidelity DNA Polymerase for Libra (Vazyme, Nanjing, China) and VIGS vectors were constructed using ClonExpress Ultra One Step Cloning Kit V2 (Vazyme, Nanjing, China).

2.10. Agrobacterium preparation and infestation

The Agrobacterium tumefaciens GV3101 cells harboring *TRV2::0*, *TRV2::HaCIPK18, TRV2::HaCIPK19* construct were cultivated in liquid LB medium at 28 ∘C overnight. After centrifugation, the bacteria were suspended by infiltration medium and adjusted OD600–0.8. The Agrobacterium tumefaciens GV3101 cells carrying TRV1 construct mixed with bacteria containing *TRV2::0, TRV2::HaCIPK18, TRV2::HaCIPK19* constructs at 1:1 ratio, respectively. The mixture was gently incubated at 28 ∘C, 60 rpm for 1 h, and then infiltrated into the cotyledon of 3–4 leafstage sunflower seedlings. The infiltrated seedlings were placed in the illumination incubator with the condition of 20 ∘C for 48 h without light. Then, the seedlings grew under the condition of 25 ∘C, 60 % relative humidity, and photoperiod 16 h light/8 h dark without light.

2.11. Virus-induced gene silencing (VIGS) assay

Agrobacterium tumefaciens GV3101 strains harboring pTRV1, pTRV2::0, pTRV2::HaCIPK18, or pTRV2::HaCIPK19 were cultured in LB medium (28°C, 200 rpm). Cells were resuspended in infiltration buffer (10 mM $MgCl_2$, 10 mM MES, 200 μM acetosyringone; OD_{600} = 0.8). pTRV1 and each pTRV2 construct were mixed (1:1) and incubated (28°C, 1 h). The mixture was infiltrated into cotyledons of 1-week-old sunflower seedlings. Plants were kept in darkness (48 h, 20°C), then transferred to 25°C (60 % RH, 16-h light/8-h dark).

2.12. Salt stress treatment

Sunflower seedlings that had been transiently transformed were transplanted into sterilised culture containers containing 1/5 Hoagland's nutrient solution. Following a 14-day hydroponic cultivation period, the seedlings had grown two rounds of true leaves. At this point, they were transferred to a hydroponic environment containing 200 mM NaCl for cultivation. Samples were collected and preserved at 0 h, 3 h, and 6 h of the salt treatment for subsequent storage, with the objective of establishing a sufficient sample reserve for experimental procedures such as RNA extraction.

2.13. NBT staining assay

Prepare 1 mg/mL of NBT staining solution (pH 7.6) at room temperature and protected from light. Control and transiently transformed sunflower leaves silenced with *HaCIPK18* that had been transiently treated with 200 mM NaCl, as well as untreated leaves of both sunflower species, were immersed in the staining solution and stained overnight in a dark environment. After staining was completed, chlorophyll was removed using 95 % ethanol. Finally, the samples were photographed by a microimaging system and the proportion of stained area to the total leaf area was calculated using ImageJ software.

2.14. DAB staining assay

A 1 mg/mL DAB chromogenic solution (pH 3.8) was prepared at 37°C. The control and sunflower leaves that had been transiently treated with 200 mM NaCl and silenced by transient transformation of HaCIPK18, as well as the two untreated sunflower leaves, were immersed in the staining solution and placed in a dark environment for 12 h. Decolourisation was completed using 95 % ethanol. The H_2O_2-specific staining phenomenon was observed using a light microscope, and the percentage of the stained area in the leaf was calculated by the image analysis software ImageJ.

2.15. Yeast two-hybrid analysis

The yeast two-hybrid system was used to screen for reciprocal proteins of HaCIPK18. *HaAKT2, HaCBL2, HaCBL3, HaCBL4, HaCBL5, HaCBL8, HaCBL10, HaCBL11, HaCBL12*, and *HaCBL13* were cloned and inserted into the pGADT7 vector, respectively, and then the recombinant completed plasmids were co-transfected with the pGBKT7-HaCIPK18 plasmid, respectively, into AH109 Saccharomyces cerevisiae strain, and the colony growth was observed after growth on double-deficient medium (SD/-Trp/-Leu) and quadruple-deficient selective medium (SD/-Trp/-Leu/-His/-Ade).

2.16. Luciferase complementation imaging assay

Tobacco seedlings were cultivated in a light incubator set at a constant temperature of 25°C, using a photoperiodic cycle of 16 h of light/8 h of darkness. One Tobacco plant was planted per pot and cultured continuously for 4–5 weeks until the plants were mature. A single colony of Agrobacterium grown on a resistant plate was picked and inoculated into 5 mL of LB liquid medium containing Kanamycin and Rifampin antibiotic, and incubated overnight at 28°C with oscillation at 220 rpm until the OD_{600} value of the bacterial solution reached 0.5–0.6. At 4000 rpm, centrifuge for 10 min, collect the bacterial bodies, discard the supernatant, resuspend the mixed bacterial solution with leachate (10 mM MES, 10 mM $MgCl_2$, 150 μM acetosyringone, pH = 5.6), centrifuge again, resuspend, and repeat for 2–3 times in order to remove the residual LB medium completely; finally, adjust the concentration of the bacterial solution with the appropriate amount of leachate to OD_{600} = 1.0, and incubate at 28°C for 2–3 h. Agrobacterium carrying recombinant plasmid HaCIPK18-nLUC and Agrobacterium carrying recombinant plasmid HaCBL10-cLUC were mixed in a ratio of 1:1, and each combination of mixed bacterial fluids had a total OD_{600} of 0.5, and the volume was replenished to 1 mL with the dip solution.

3. Results

3.1. Identification and analysis of CIPK family in sunflowers

A comprehensive analysis of the sunflower genome allowed us to identify 36 *CIPK* genes, which are distributed across 16 of the sunflower's 17 chromosomes (Table 1). Chromosomal mapping revealed uneven distribution, with chromosomes 4 and 11 harboring the highest density (5 genes each), while chromosome 7 lacked *CIPK* genes entirely (Fig. 1A).

Analysis of *HaCIPK* gene structures revealed substantial variation in exon-intron organization (Fig. 1B). Exon numbers ranged from 6 to 15, with *HaCIPK5* having the most complex structure (15 exons and 14 introns). Syntenic analysis identified 9 duplicate *HaCIPK* gene pairs (Fig. 1C), comprising 7 segmental and 2 tandem duplication events, indicating duplication-driven expansion of this family.

To further investigate the characteristics of *HaCIPK* family members, we analyzed the physicochemical properties of the 36 HaCIPK proteins (Table 1). The amino acid length of these HaCIPK proteins ranges from 257 (HaCIPK23) to 545 (HaCIPK11), and their corresponding molecular weights range from 29217.72 (HaCIPK23) to 62172.92 (HaCIPK11). The theoretical isoelectric points (pI) of HaCIPK proteins range from 6.15 (HaCIPK32) to 9.14 (HaCIPK7). Among these 36 proteins, 6 are acidic, and the remaining 30 are basic.

3.2. Phylogenetic and collinearity analysis of CIPK family members in different species

To characterize the *CIPK* family across species, we identified 90 CIPK proteins from *Arabidopsis thaliana* (26), *Oryza sativa* (32), and *Lactuca sativa* (32) (Fig. 2B). To further explore the evolutionary relationships of *CIPK* family members, we constructed a phylogenetic tree by comparing the CIPK proteins from these three species and sunflower. The analysis revealed that the CIPK proteins can be classified into four major clades (Group I-IV) based on their homology (Fig. 2A). Group I contains 42 proteins, group II 16, group III 31, and group IV 35, which gives a comprehensive overview of the family's evolutionary characteristics. Phylogenetic classification demonstrated differential clustering of

Table 1
Basic physical and chemical properties and predicted subcellular localisation of the sunflower CIPK protein.

Gene ID	Gene name	Number of Amion Acid	Molecular weight(Da)	Isoelectric point (IP)	Most Likely location	Instability index	Aliphatic index	Grand average of hydropathicity
HanXRQr2_Chr01g0000011	*HaCIPK1*	449	50750.15	6.50	Cytoplasm	35.48	93.30	−0.249
HanXRQr2_Chr01g0018941	*HaCIPK2*	430	48743.13	8.49	Chloroplast	44.52	90.84	−0.322
HanXRQr2_Chr01g0018981	*HaCIPK3*	448	51166.29	9.14	Cytoplasm	35.88	91.63	−0.427
HanXRQr2_Chr02g0068761	*HaCIPK4*	447	50613.02	6.48	Cytoplasm	35.86	90.87	−0.278
HanXRQr2_Chr03g0093441	*HaCIPK5*	429	48074.43	9.20	Cytoplasm	35.85	82.96	−0.317
HanXRQr2_Chr03g0126281	*HaCIPK6*	451	50801.04	7.57	Chloroplast	30.40	80.64	−0.365
HanXRQr2_Chr03g0136771	*HaCIPK7*	435	48932.50	9.14	Chloroplast	36.62	86.39	−0.348
HanXRQr2_Chr04g0145031	*HaCIPK8*	451	51273.18	8.92	Nucleus	39.89	81.04	−0.363
HanXRQr2_Chr04g0159731	*HaCIPK9*	447	50936.72	8.70	Cytoplasm	34.22	86.17	−0.505
HanXRQr2_Chr04g0173171	*HaCIPK10*	455	51063.94	8.93	Chloroplast	34.73	87.41	−0.294
HanXRQr2_Chr04g0174651	*HaCIPK11*	545	62172.92	8.81	Cytoplasm	49.43	91.14	−0.242
HanXRQr2_Chr04g0174661	*HaCIPK12*	448	50299.38	6.74	Cytoplasm	33.06	93.57	−0.176
HanXRQr2_Chr05g0203811	*HaCIPK13*	426	47547.89	9.01	Cytoplasm	35.61	83.78	−0.282
HanXRQr2_Chr05g0218961	*HaCIPK14*	452	50859.18	6.58	Nucleus	35.84	91.62	−0.392
HanXRQr2_Chr06g0264621	*HaCIPK15*	453	51317.19	8.50	Cytoplasm	34.59	90.38	−0.232
HanXRQr2_Chr06g0267311	*HaCIPK16*	438	49283.89	8.95	Cytoplasm	39.64	88.33	−0.236
HanXRQr2_Chr08g0344691	*HaCIPK17*	428	48307.88	8.87	Cytoplasm	43.81	93.57	−0.230
HanXRQr2_Chr09g0371011	*HaCIPK18*	432	48597.35	9.06	Cytoplasm	38.67	84.14	−0.265
HanXRQr2_Chr09g0383201	*HaCIPK19*	429	48713.52	8.99	Cytoplasm	28.37	84.29	−0.367
HanXRQr2_Chr09g0413881	*HaCIPK20*	447	50522.28	8.75	Cytoplasm	38.09	80.65	−0.294
HanXRQr2_Chr10g0460981	*HaCIPK21*	426	48080.79	8.78	Chloroplast	31.95	87.84	−0.280
HanXRQr2_Chr11g0493581	*HaCIPK22*	442	50168.86	7.62	Chloroplast	37.54	92.87	−0.346
HanXRQr2_Chr11g0493651	*HaCIPK23*	257	29217.72	6.38	Chloroplast	34.12	90.62	−0.102
HanXRQr2_Chr11g0501071	*HaCIPK24*	409	45141.49	8.09	Chloroplast	31.91	100.54	−0.028
HanXRQr2_Chr11g0501111	*HaCIPK25*	435	49680.33	8.66	Cytoplasm	31.05	95.15	−0.272
HanXRQr2_Chr11g0502731	*HaCIPK26*	473	53732.75	8.57	Chloroplast	48.26	87.32	−0.341
HanXRQr2_Chr12g0554121	*HaCIPK27*	435	49153.81	8.94	Chloroplast	40.53	92.76	−0.300
HanXRQr2_Chr13g0614451	*HaCIPK28*	441	49582.70	8.91	Chloroplast	34.88	90.57	−0.248
HanXRQr2_Chr14g0631891	*HaCIPK29*	439	50066.64	7.66	Chloroplast	37.44	84.62	−0.401
HanXRQr2_Chr15g0695271	*HaCIPK30*	454	51092.85	8.88	Chloroplast	40.66	86.76	−0.354
HanXRQr2_Chr15g0720431	*HaCIPK31*	433	48741.62	8.53	Cytoplasm	27.36	87.76	−0.227
HanXRQr2_Chr16g0743001	*HaCIPK32*	434	49333.44	6.15	Cytoplasm	39.34	85.35	−0.343
HanXRQr2_Chr16g0758121	*HaCIPK33*	463	52610.78	9.14	Chloroplast	29.39	81.30	−0.432
HanXRQr2_Chr16g0758141	*HaCIPK34*	465	52960.99	8.61	Chloroplast	44.99	89.68	−0.278
HanXRQr2_Chr17g0817341	*HaCIPK35*	482	54802.25	8.59	Chloroplast	38.96	88.30	−0.228
HanXRQr2_Chr17g0822011	*HaCIPK36*	476	54057.96	8.80	Chloroplast	38.36	79.05	−0.488

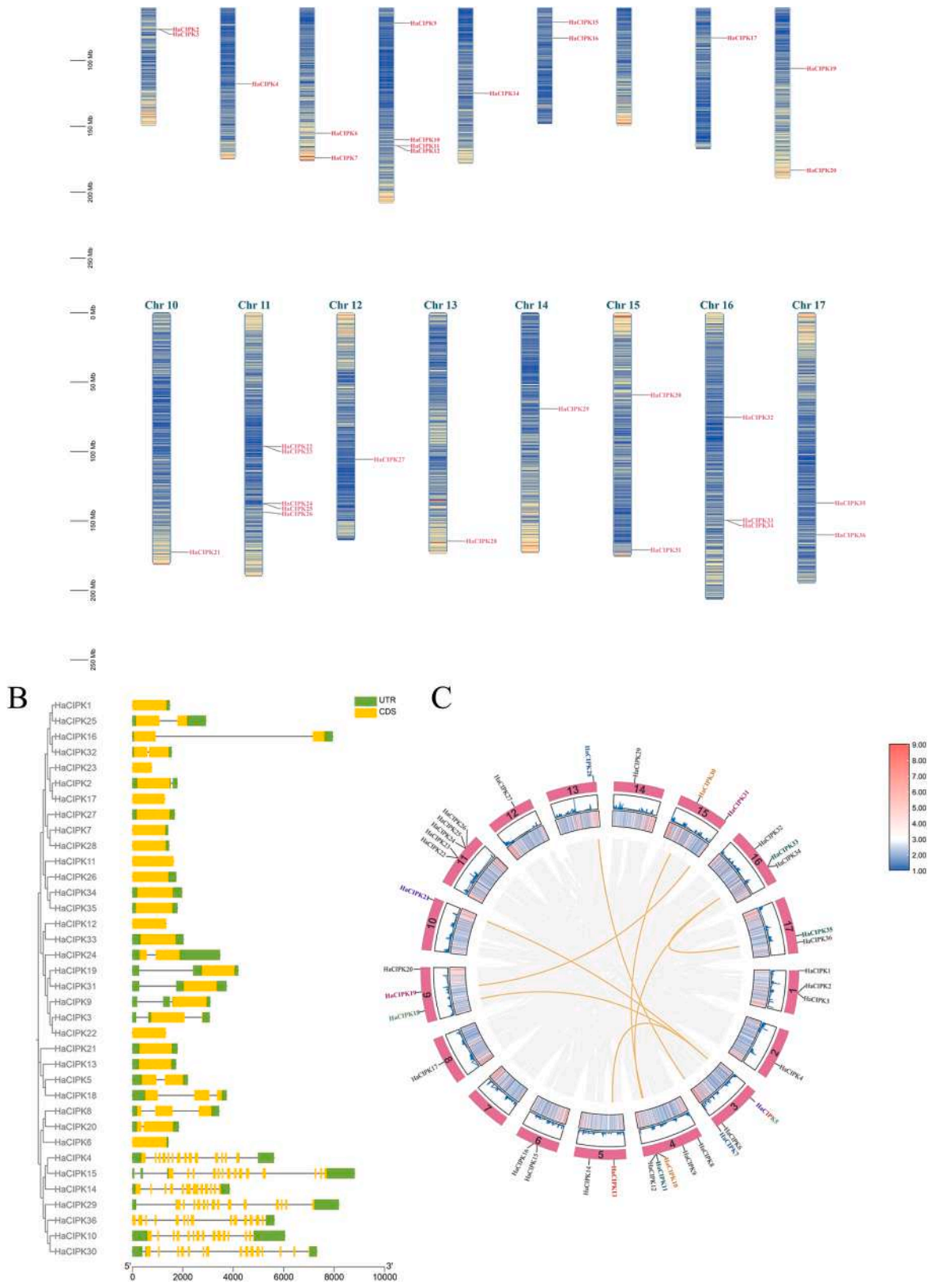

Fig. 1. Identification and characterization of *CIPK* family genes in sunflower.(A) Localization of HaCIPK genes on chromosomes. Chromosome lengths are labeled on the left in Mb.(B) Phylogenetic tree and gene architecture of the sunflower CIPK family. The evolutionary relationships of 36 HaCIPK genes were analyzed by drawing evolutionary trees, and the exon-intron structures of their untranslated regions (UTRs) and coding regions (CDSs) were mapped.(C) Syntenic analysis of *H. annuus CIPK* genes. The figure shows the distribution of the 36 HaCIPK genes on the sunflower chromosomes and depicts the homologous relationships between gene pairs by connecting the yellow lines.

A

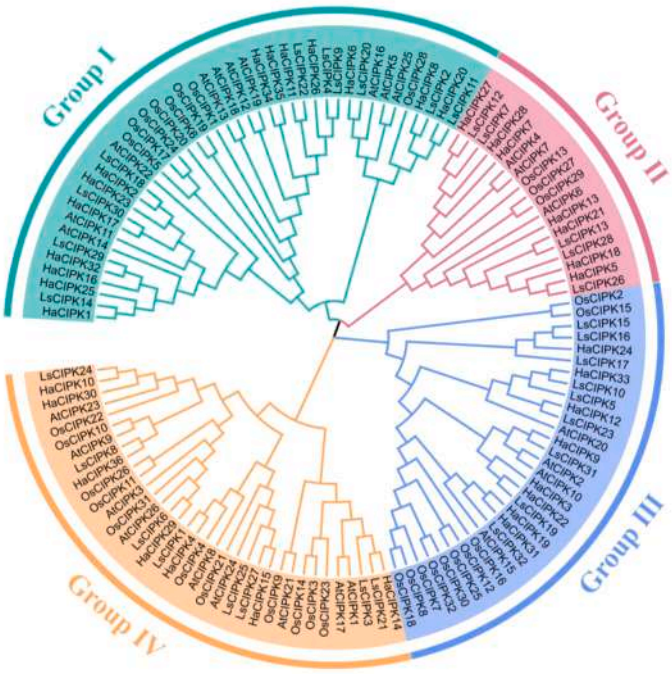

B

Species	Total	GroupI	GroupII	GroupIII	GroupIV
A.thaliana	26	10	3	4	9
O.sativa	32	8	3	10	11
L.sativa	32	10	5	9	8
H.annuus	36	14	5	8	7

Fig. 2. Phylogenetic analysis and classification of CIPK proteins across 4 species.(A) Phylogenetic analyses of CIPK proteins of *Helianthus annuus*, *Arabidopsis thaliana*, *Oryza sativa,* and *Lactuca sativa*. All CIPK proteins within the four species were categorized into four groups according to correlation, and each group is represented by green, pink, blue and orange colors. (B) Taxonomic distribution of CIPK proteins among the analyzed plant species.

HaCIPK genes, with distinct allocation across evolutionary clades: 14 in group I, 5 in group II, 8 in group III, and 7 in group IV.

To further understand the homology between sunflower *CIPK* genes and those of the other three species, we performed an interspecies synteny analysis by comparing the sunflower *CIPK* gene family with that of the other three species (Fig. 2C). This analysis revealed that 14, 20, and 6 *CIPK* genes from *Arabidopsis thaliana*, *Lactuca sativa* and *Oryza sativa*, respectively, share collinear sequences with sunflower *CIPK* family members.

3.3. Conserved motif and domain architecture of the CIPK family

To better understand the structural domain features of the 126 *CIPK* family members, we analyzed their motif distributions by using the Multiple Expectation Maximization for Motif Elicitation (MEME) suite. This analysis identified eight conserved motifs in the CIPK family (Figure S2A), and these motifs range in length from 14 to 50 amino acids. The specific sequences and compositions of these eight motifs are provided in Figure S3.

Across the four species, the motif distribution of the CIPK gene family is highly conserved. Further structural domain analyses showed that, with the exception of *HaCIPK23* which contains only the Pkinase structural domain, all other CIPK family members feature both the Pkinase and NAF structural domains. The Pkinase domain was made up of motifs 1–5 and 8, while motifs 6 and 7 form the core of the NAF structural domain (Figure S2A and S2B).

3.4. Cis-Regulatory Element Profiling in CIPK Promoters

To investigate the transcriptional regulation of *CIPK* genes, we analyzed the promoters of these genes. We extracted 2000-bp upstream sequences of *CIPK* family genes from the four species, then analyzed these sequences for *cis*-elements via the PlantCARE database. We identified nine *cis*-regulatory elements, which were associated with drought tolerance, defense and stress resistance, MeJA response, ABA response, auxin response, salicylic acid response, gibberellin response, and low-temperature adaptation (Fig. 3A).

Notably, statistical analysis showed that MeJA-responsive elements, ABA-responsive elements, and low-temperature-inducible elements were the most abundant in the promoters of these *CIPK* genes, with 580, 422, and 132 occurrences, respectively (Fig. 3C). Furthermore, *H. annuus* promoters have the highest density of all *cis*-element types among the four species (Fig. 3B), which suggests enhanced regulatory complexity in sunflower *CIPKs*.

3.5. Stress-responsive expression profiles of HaCIPK genes

Since sunflower is recognized as a pioneering crop in saline soils, exploring the role of CIPK family genes in salt stress responses is critical. Therefore, we analyzed RNA-seq data from salt-treated sunflower seedlings to collate and analyze the expression profiles of all 36 *HaCIPK* genes (Fig. 4A). The expression levels of *HaCIPK18* and *HaCIPK19* were substantially elevated in both roots and leaves after salt stress. In order to clarify the transcriptional expression pattern of *HaCIPK18* and

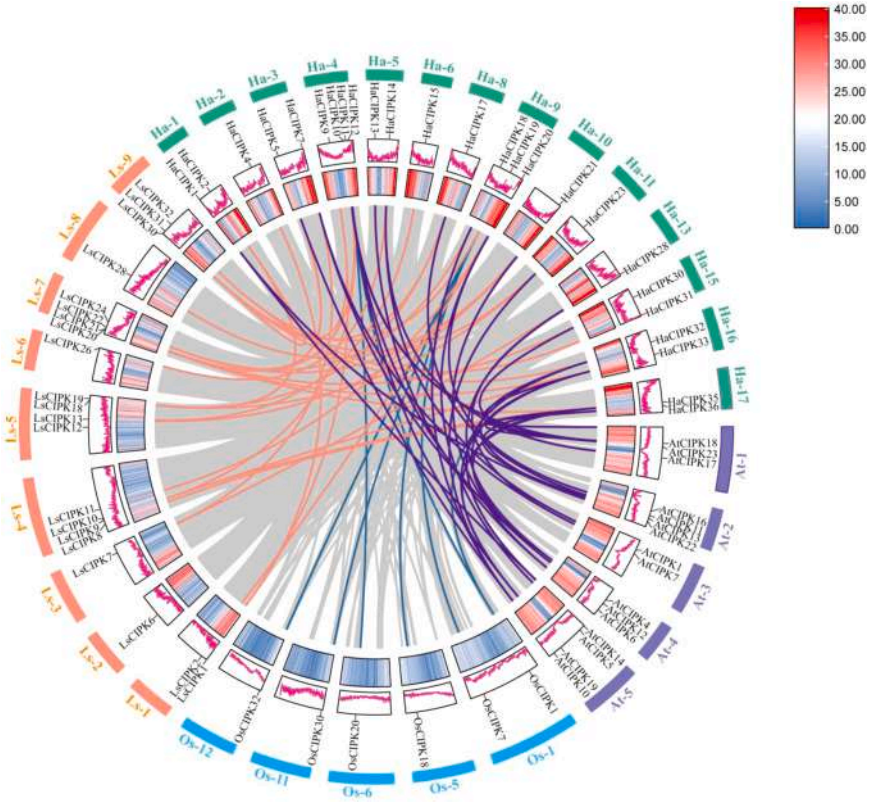

Fig. 3. Syntenic analysis of CIPK proteins between Helianthus annuus(sunflower) and other three species(Arabidopsis thaliana, Oryza sativa, Lactuca sativa).

HaCIPK19 after salt stress, the transcriptional expression levels of *HaCIPK18* and *HaCIPK19* were examined in sunflower subjected to different times of salt stress using qRT-PCR technology. Further qRT-PCR analysis showed that *HaCIPK18* expression peaked after 9 h of salt treatment, while *HaCIPK19* expression reached its highest point after 6 h of salt treatment (Fig. 4B and C).

3.6. *HaCIPK18 confers salt stress tolerance in sunflower*

To functionally characterize *HaCIPK18* and *HaCIPK19* in salt adaptation, we employed virus-induced gene silencing (VIGS) to create sunflower lines with *HaCIPK18* or *HaCIPK19* silenced. Quantitative RT-PCR confirmed efficient silencing of *HaCIPK18* and *HaCIPK19* in the gene-silenced sunflowers (>85 % reduction) (Fig. 5C and S4B).

Under normal conditions, no significant differences were observed between *HaCIPK18*-silenced and *HaCIPK19*-silenced sunflowers compared to the control (VI::0) (Fig. S4E-G and S5C-E). For salt stress treatments, we set 3 biological replicates per line, with 8 seedlings per replicate; after 7 days of 200 mM NaCl exposure, we evaluated phenotypes (via grading), performed NBT/DAB staining, and measured fresh weight and relative water content (RWC). When subjected to salt treatment, the *HaCIPK18*-silenced plants (VI::*HaCIPK18*) exhibited significant salt sensitivity compared to the control (Fig. 5A and B). We graded leaf wilting into four categories: Grade I indicates no obvious leaf wilting, Grade II means only leaf tips are wilted, Grade III represents obvious wilting covering less than 50 % of the leaf area, and Grade IV denotes severe wilting with over 50 % of the leaf area affected. Following salt treatment, true leaf necrosis was more severe in the *VI::HaCIPK18*-silenced lines than in the control (Fig. 5D). In contrast, *HaCIPK19*-silenced plants showed no discernible salt sensitivity (Fig. S4A).

Physiological analyses revealed that *HaCIPK18* depletion exacerbated salt-induced oxidative damage. To directly assess O^{2-} accumulation under salt treatment, we stained leaves from the *HaCIPK18*-silenced lines and the *VI::0* strain with NBT and DAB. The staining results revealed that the average intensity of NBT and DAB staining in the leaves of the *HaCIPK18*-silenced lines with or without salt treatment, was significantly higher than that of the control group (Fig. 6A and B). This suggests that *HaCIPK18* plays a role in reducing leaf damage in plants and possesses strong antioxidant properties.

Additionally, we measured the water loss rate and fresh weight of the *VI::HaCIPK18*-silenced lines before and after salt treatment. The *VI::HaCIPK18*-silenced sunflowers exhibited a significantly lower relative water content and a significantly lower fresh weight after salt treatment (Figs. 5E and 5F). These collective findings establish *HaCIPK18* as a critical regulator of salt tolerance through mitigation of oxidative stress and maintenance of cellular hydration.

3.7. *The expression pattern of HaCIPK18*

In order to systematically analyse the spatial and temporal expression characteristics of the *HaCIPK18* gene in sunflower, five key developmental periods (germination, seedling stage I and II, present bud stage and flowering stage) were selected for tissue-specific analysis in this study. The gene expression levels were detected by extracting total RNA from different tissue samples in each period and using quantitative real-time PCR. The results showed that *HaCIPK18* was mainly expressed in different tissues at different periods, mainly in cotyledons at germination, in newborn true leaves at seedling stage I, in roots at seedling stage II, in buds at budbreak, and in styles at flowering stage (Fig. 7). Combined with the above results, it was hypothesised that the gene had different spatial and temporal expression characteristics in various tissues of sunflower, and that it was mainly expressed in roots at seedling stage II, suggesting that it possesses early salt resistance. In addition, the high expression of this gene in the style during the flowering stage suggests that it may play a key role in the development of sunflower reproductive organs and the accumulation of seed nutrients.

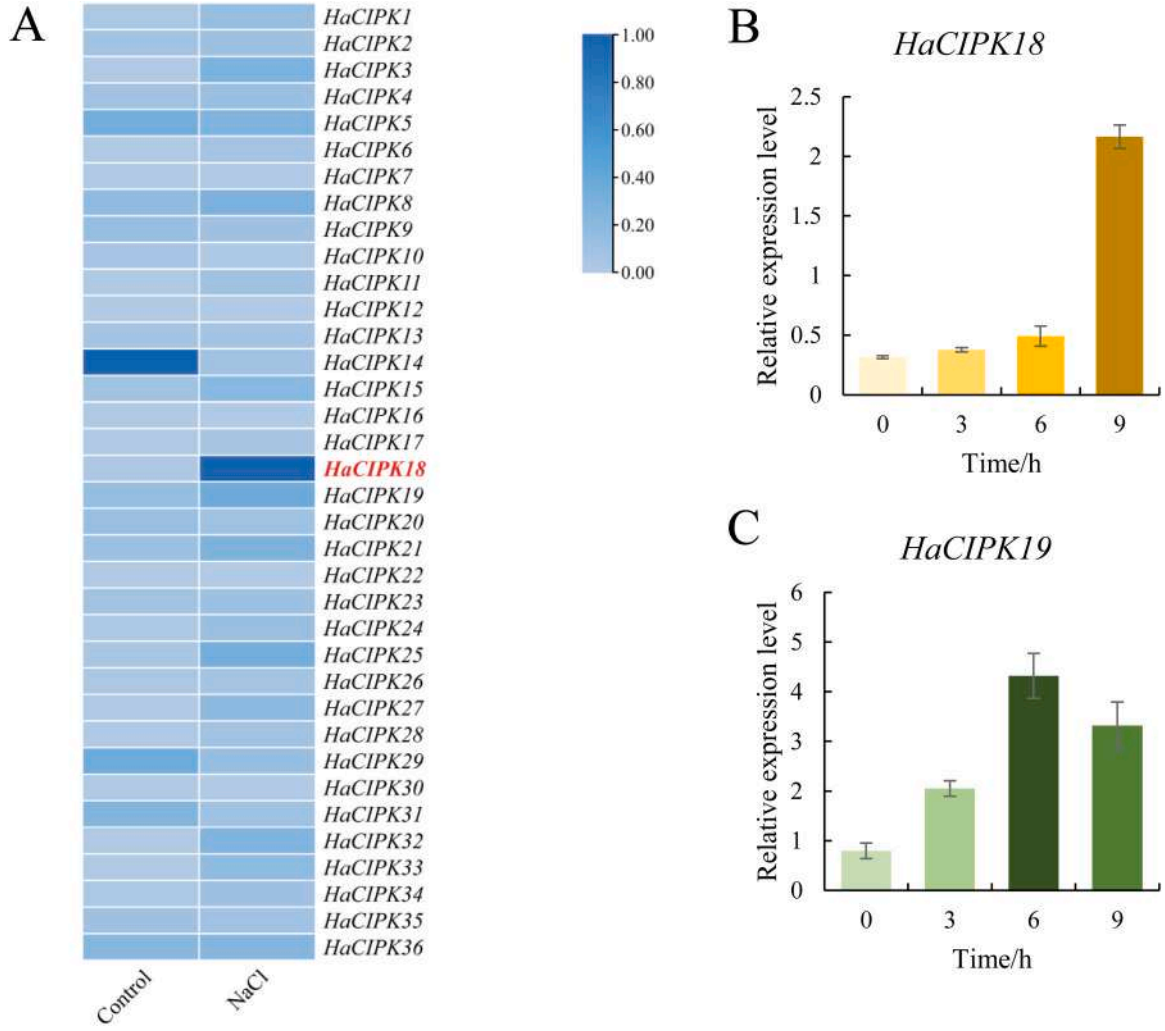

Fig. 4. Expression pattern analysis of HaCIPK genes.(A) Heat map of HaCIPKs expression in different tissues under salt stress. (B,C) qRT-PCR analysis of HaCIPK18 (B) and HaCIPK19 (C) expression in sunflower leaves at 0, 3, 6, and 9 h after 200 mM NaCl treatment. Data are presented as Mean ± SD (n = 3 biological replicates). Different lowercase letters indicate significant differences between time points (one-way ANOVA, Duncan's test, $P < 0.05$).

3.8. Screening and validation of HaCIPK18-interacting proteins

Fourteen *CBL* gene family members were identified in the whole genome of sunflower by BLASTP algorithm and HMM modeling method and renamed according to their positions on sunflower chromosomes. Expression patterns of sunflower *CBL* family members under salt stress were identified based on transcriptome data from the NCBI SRA database, and the transcript expression levels of *HaCBL2, HaCBL3, HaCBL4*, and *HaCBL10* were found to be significantly elevated in response to salt stress induction, suggesting that these genes may be involved in salt response(Fig. 8A). The CBL family members *HaCBL2, HaCBL3, HaCBL4, HaCBL5, HaCBL8, HaCBL10, HaCBL11, HaCBL12, HaCBL13*, and the gene encoding a potassium channel protein, *HaAKT2* (a homolog of *AtAKT2*) were cloned from the sunflower autologous material, AZB, and were recombinantly ligated into the pGADT7 vector. pGADT7 vector and co-transfected with pGBKT7-HaCIPK18 plasmid into yeast. The results showed that all these recombinant yeasts grew normally on double-deficient medium, while only HaCBL10 interacted with HaCIPK18 on quadruple-deficient medium(Fig. 8B).

To further validate that the protein kinase HaCIPK18 is able to interact with the calmodulin-like protein HaCBL10, protein interactions need to be visualised by luciferase complementation imaging (LCI) experiments. The fusion proteins, nLUC-HaCIPK18 and cLUC-HaCBL10, were co-expressed in tobacco leaves. The results showed that the area of the experimental group where the two fusion proteins were co-expressed showed stronger fluorescence signals than the area of the control group(Fig. 8C). This confirms that HaCIPK18 can interact with HaCBL10.

3.9. Expression analysis of salt response-related genes in sunflower after silencing HaCIPK18

To elucidate *HaCIPK18*'s role in salt signaling, we compared transcript profiles of the VIGS-silenced (*VI*::*HaCIPK18*) and control (*VI*::*0*) plants under salt stress. qRT-PCR analysis of 12 salt-responsive genes showed that while all these genes were induced by NaCl treatment in both genotypes, six key regulators, *HaDREB2A*, *HaRD22*, *HaLEA18*, *HaLEA1-A*, *HaSOS2,* and *HaGORK*, had significantly attenuated induction levels in *HaCIPK18*-silenced plants compared to controls (Fig. 9). This selective suppression of stress-responsive transcriptional activation suggests HaCIPK18 may act upstream in the salt adaptation signaling network, and potentially help coordinate the expression of effector genes. These effector genes likely play critical roles in ion homeostasis (*HaSOS2*, *HaGORK*) and cellular protection (HaLEAs, HaRD22), which further supported the hypothesis that *HaCIPK18* contributes to enhancing salt tolerance in sunflower. However, the specific molecular mechanisms through which HaCIPK18 regulates these downstream genes still need further verification.

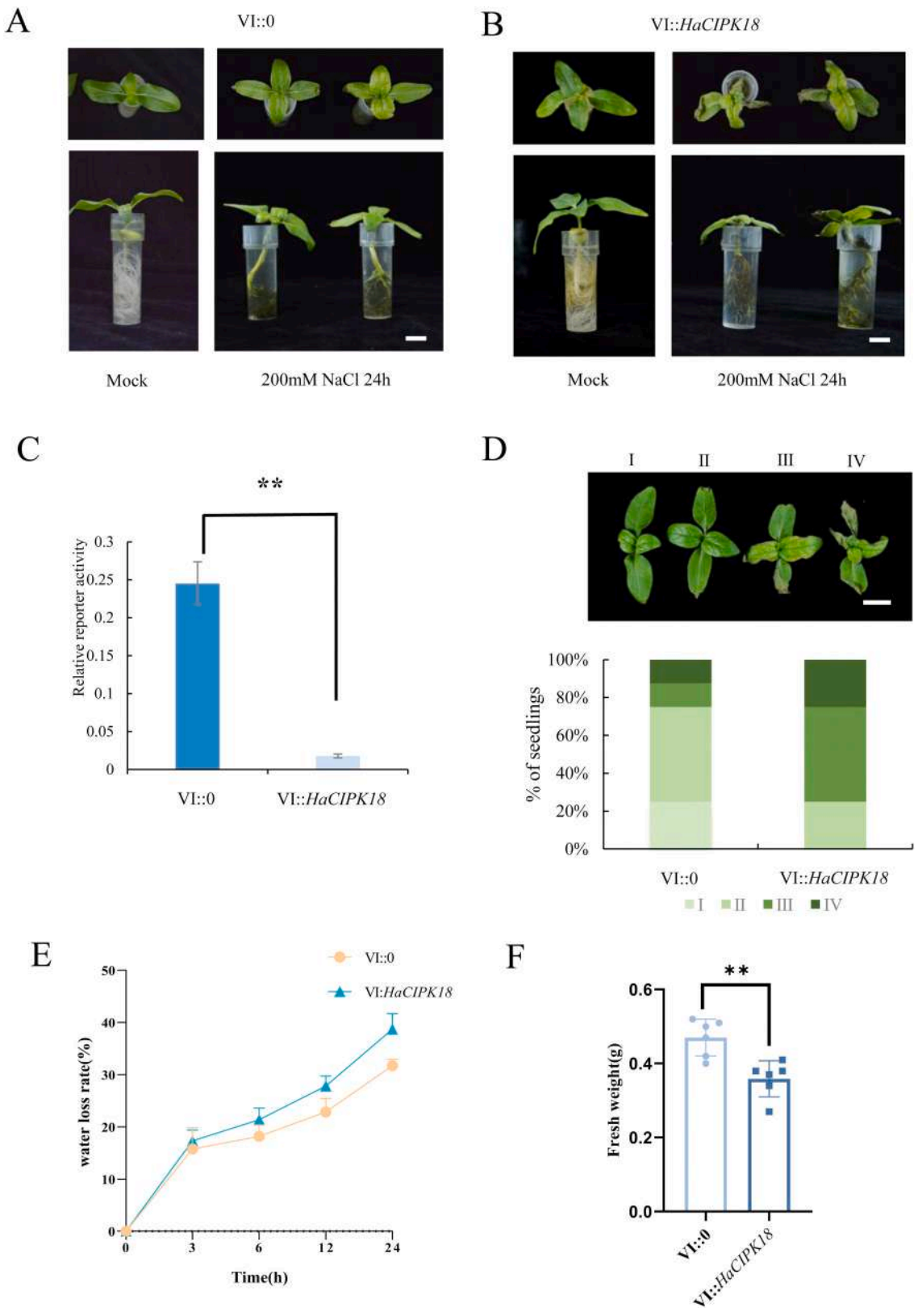

Fig. 5. Silencing of HaCIPK18 reduces salt tolerance in sunflower seedlings.(A,B) Phenotypes of sunflower VIGS silencing HaCIPK18 (VI::HaCIPK18) seedlings versus empty vectors (VI::0) after treatment with 200 mM NaCl for 24 h after 14 days of culture. Untreated seedlings served as controls. scale bar is 1 cm, ** indicates $P < 0.01$ (C)qPCR validation of VIGS efficiency.(D) Leaf damage grading statistics of VI::0 and VI::HaCIPK18 after treatment with 200 mM NaCl for 24 h.(E) Water loss rate of two-week-old VIGS sunflower seedlings and empty vectorsand (F)flesh weight of two-week-old VIGS sunflower seedlings and empty vectors after two days of 200 mM NaCl treatment., ** indicates $P < 0.01$.

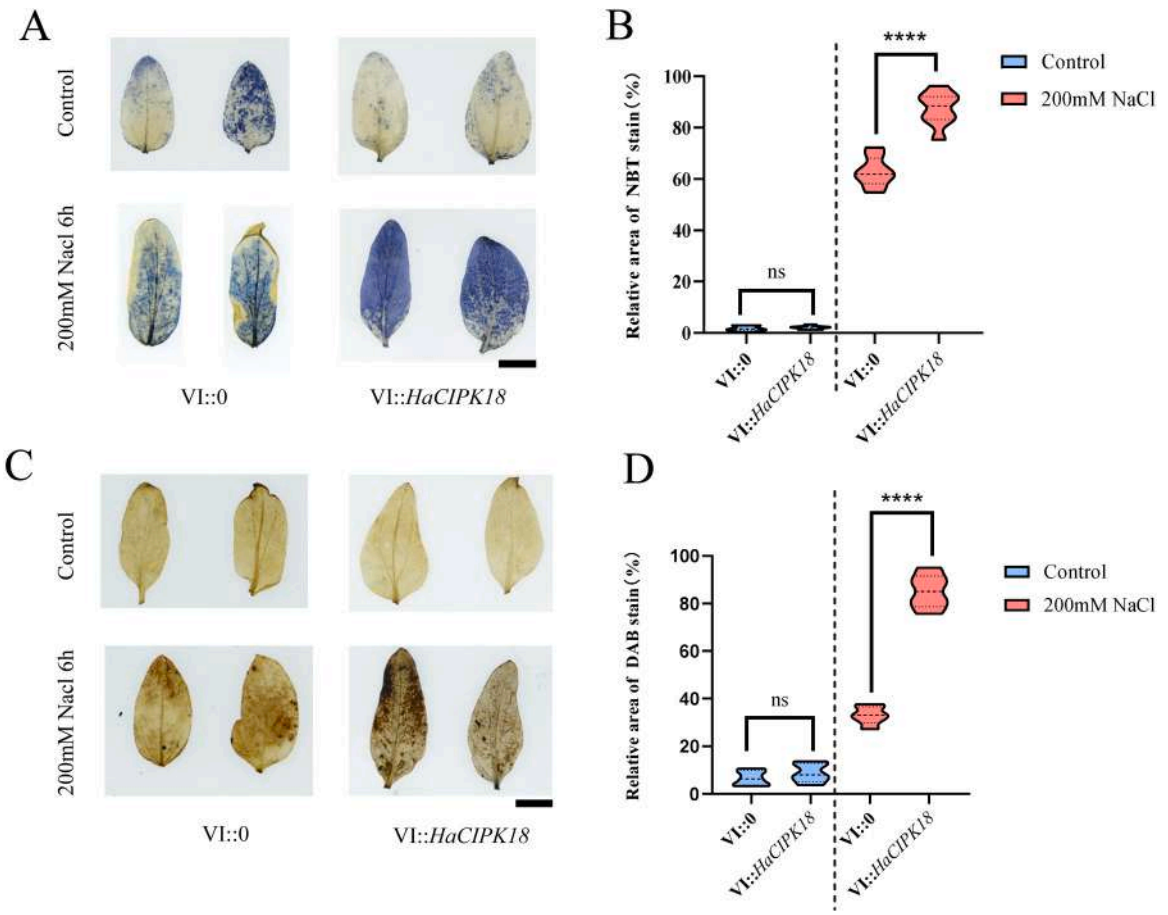

Fig. 6. Determination of reactive oxygen species levels in HaCIPK18 gene-silenced lines. (A)NBT staining of sunflower leaves, scale bar is 1.5 cm, Control indicates untreated; (B) relative area of NBT stained area of sunflower leaves; (C) DAB staining of sunflower leaves, scale bar is 1.5 cm; (D) relative area of DAB stained area of sunflower leaves, ns indicates $P > 0.05$, **** indicates $P < 0.0001$.

4. Discussion

4.1. The HaCIPK family mediates multifaceted stress adaptation

Previous studies have demonstrated that the *CIPK* family plays a crucial role in regulating plant responses to abiotic stresses. The involvement of the *CIPK* family in salt stress responses was among the earliest to be characterized. Our findings establish *HaCIPK18* as a positive regulator of salt tolerance in sunflower, consistent with the conserved roles of CIPKs in abiotic stress signaling across plant species. The observed salt-induced *HaCIPK18* upregulation and hypersensitivity of VIGS-silenced lines (Fig. 5A-F) mirror mechanisms in rice(Qin et al., 2024), poplar (Tian et al., 2017), and pineapple (Aslam et al., 2022), where CIPKs also orchestrate ion homeostasis to enhance salt tolerance.

Beyond salt adaptation, *cis*-regulatory profiling revealed enrichment of low-temperature-responsive elements in *HaCIPK* promoters (Fig. S1), suggesting *HaCIPKs* may also function in cold adaptation. This aligns with functional reports in citrus(Xiao et al., 2022), tea (Di et al., 2024), and pepper (Ma et al., 2022), where CIPK modules enhance freezing tolerance. Similarly, drought-responsive *cis*-elements and ABA-induced expression of HaCIPK5/8/9/29/31 (Fig. 3A) suggest HaCIPKs are involved in water-deficit responses, a function paralleling roles of *StCIPK18* in potato (Yang et al., 2023) and *TaCIPK19* in wheat (Wu et al., 2023). Collectively, *HaCIPKs* likely function as signaling hubs that integrate salt, cold, and drought responses via both ABA-dependent and ABA-independent pathways.

4.2. Evolutionary conservation and divergence of CIPK gene structure

Phylogenomic analysis resolved 36 *HaCIPK* genes into four monophyletic clades (Fig. 2). Conserved kinase-NAF domain architectures (Fig. S2) further support deep evolutionary conservation, as observed in soybean(Jiao et al., 2024) and tomato(Zhang et al., 2019). Notably, gene structure divergence revealed three distinct classes: intron-rich genes (7 members with 14–15 introns), moderately spliced genes (13 with 1–2 introns), and intronless genes (16 members; Fig. 1B). This structural gradient matches reported CIPK family evolutionary patterns in other plants. Specifically, Arabidopsis thaliana CIPKs fall into two clades: the intron-rich clade and the intron-less clade. Genes with closer evolutionary relationships typically have similar functions and correlated expression, and studies indicate that both segmental duplication and tandem duplication drive the expansion of these two clades(Mao et al., 2016). The rice CIPK gene family has 8 intron-less members and 22 intron-harboring members. Among the intron-harboring members, the phase and position of introns are highly conserved with their Arabidopsis homologs. Additionally, CIPKs in both rice and Arabidopsis can form two subgroups based on sequence similarity, and the clustering of these subgroups matches perfectly with whether the genes contain introns or not. This finding indicates that in the CIPK family, the pattern where intron characteristics are linked to evolutionary clades was already established before monocots and dicots diverged (Kolukisaoglu et al., 2004, Li et al., 2009).

Based on the above evolutionary rules of CIPKs in other plants, we propose a preliminary hypothesis for the evolutionary significance of intron-less HaCIPK variants. These variants may have originated from

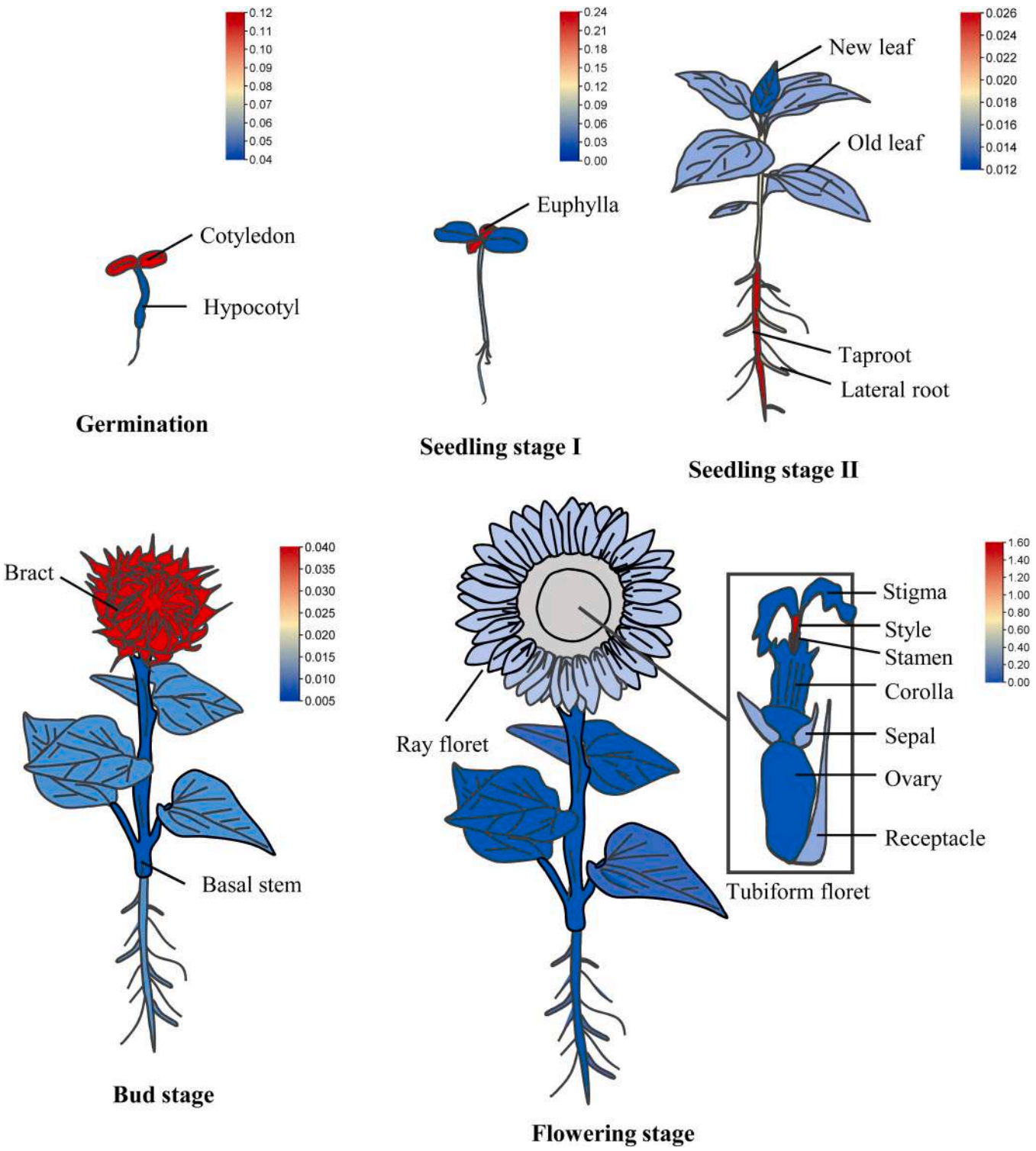

Fig. 7. Expression analysis of HaCIPK18 in different tissues at five stages (Germination stage, Seedling stage I, Seedling stage II, Bud stage, Flowering stage). Tissues include cotyledon, hypocotyl, euphylla, taproot, lateral root, new leaf, old leaf, basal stem, apical stem, bract, ray floret, and tubiform floret. HaTubulin served as the internal control.

recent retrotransposition events, a mechanism shared with intronless CIPK evolution in rice, and could potentially support stress-specific functional divergence in sunflowers. However, this hypothesis has two limitations. First, it is unclear if these variants retain CBL-interacting ability, a key trait for CIPKs to mediate stress signals. Second, their potential as truncated signaling intermediates cannot be ruled out. Both require further biochemical verification.

4.3. Spatiotemporal expression implicates HaCIPK18 in reproductive development

HaCIPK18 exhibits stage-specific expression dominance, shifting from roots during vegetative growth (20 DAP) to floral styles at anthesis (Fig. 7). While CIPKs like *AtCIPK19* (Zhu et al., 2016)and *SlCIPK9* (Martínez-Martínez et al., 2024) regulate pollen development, and

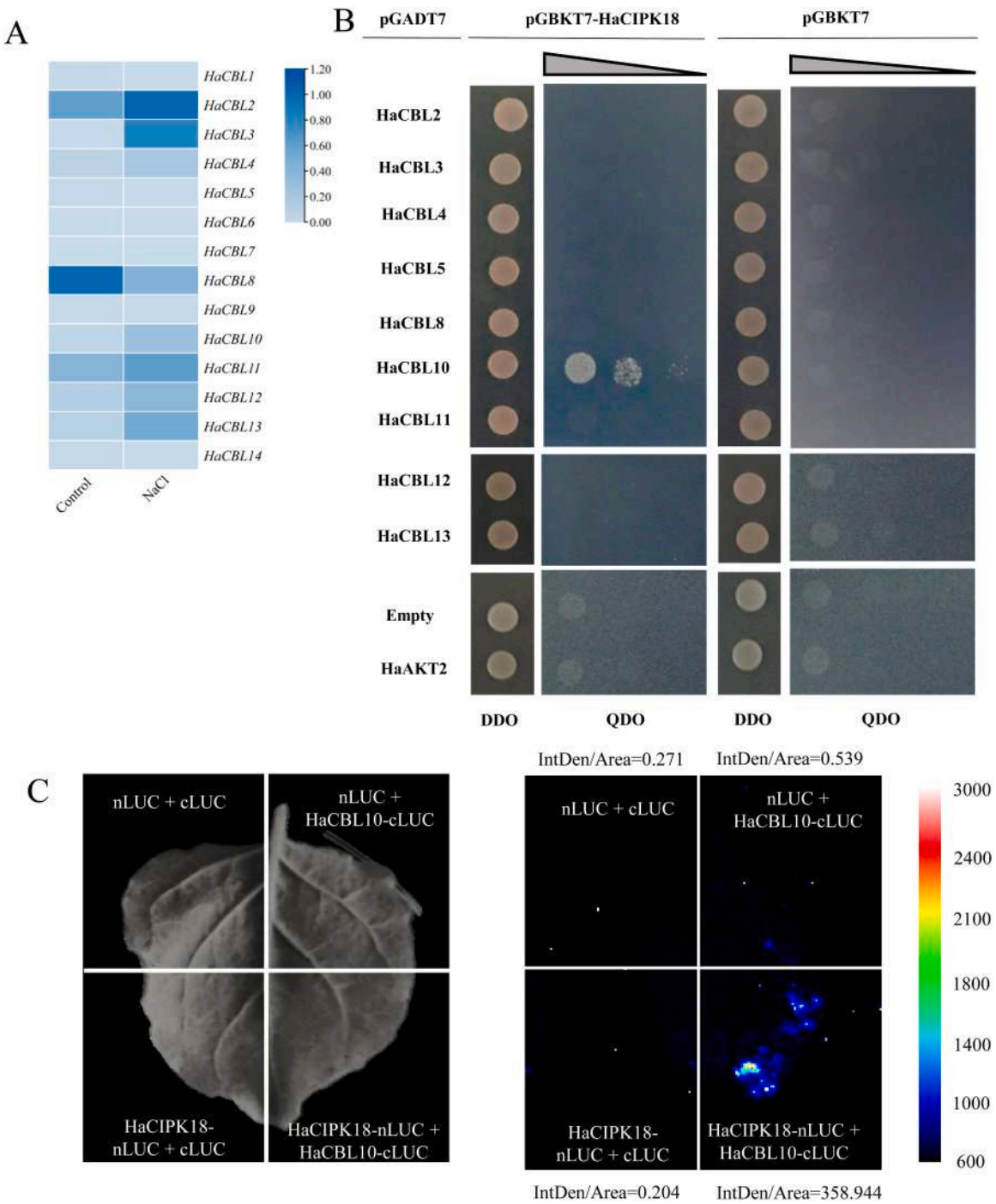

Fig. 8. Screening and validation of HaCIPK18-interacting proteins. (A) Heat map of HaCBLs expression in different tissues under salt stress.(B) Yeast two-hybrid assay to screen for HaCIPK18-interacting proteins. DDO indicates the growth of each recombinant yeast on double-deficient medium, and QDO indicates the growth of each recombinant yeast on quadruple-deficient medium, and the three concentration gradients are stock solution (100), 10–1, and 10–2, respectively. (C) Complementary luciferase imaging experiments verified HaCIPK18 and HaCBL10 interactions. Tobacco leaves was divided into four regions according to the combination of injected infestation fluids, namely, the control nLUC + cLUC region, the control nLUC + HaCBL10-cLUC region, the control HaCIPK18-nLUC + cLUC region, and the experimental HaCBL10-cLUC + HaCIPK18-nLUC region.

OsCIPK23 influences pollen fertility and seed setting in rice(Yang et al., 2008), *HaCIPK18*'s style-predominant expression pattern leads to a preliminary hypothetical inference of its potential novel roles in female reproductive tissues. This inference is further contextualized by similar tissue-specific CIPK expression patterns reported in orchid (Zhang et al., 2023) and cotton (He et al., 2013), which collectively hint at lineage-specific subfunctionalization of CIPKs in floral development.

4.4. Involvement of HaCIPK18 in possible signaling pathways for salt tolerance in sunflower

In this study, HaCBL10 was screened for interactions with HaCIPK18 by yeast two-hybrid assay, and the interactions between the two proteins were verified by luciferase complementation imaging assay (Fig. 8B and C). This finding indicates that in the sunflower, HaCIPK18 is recruited by HaCBL10 to form a complex, and that HaCBL10 receives

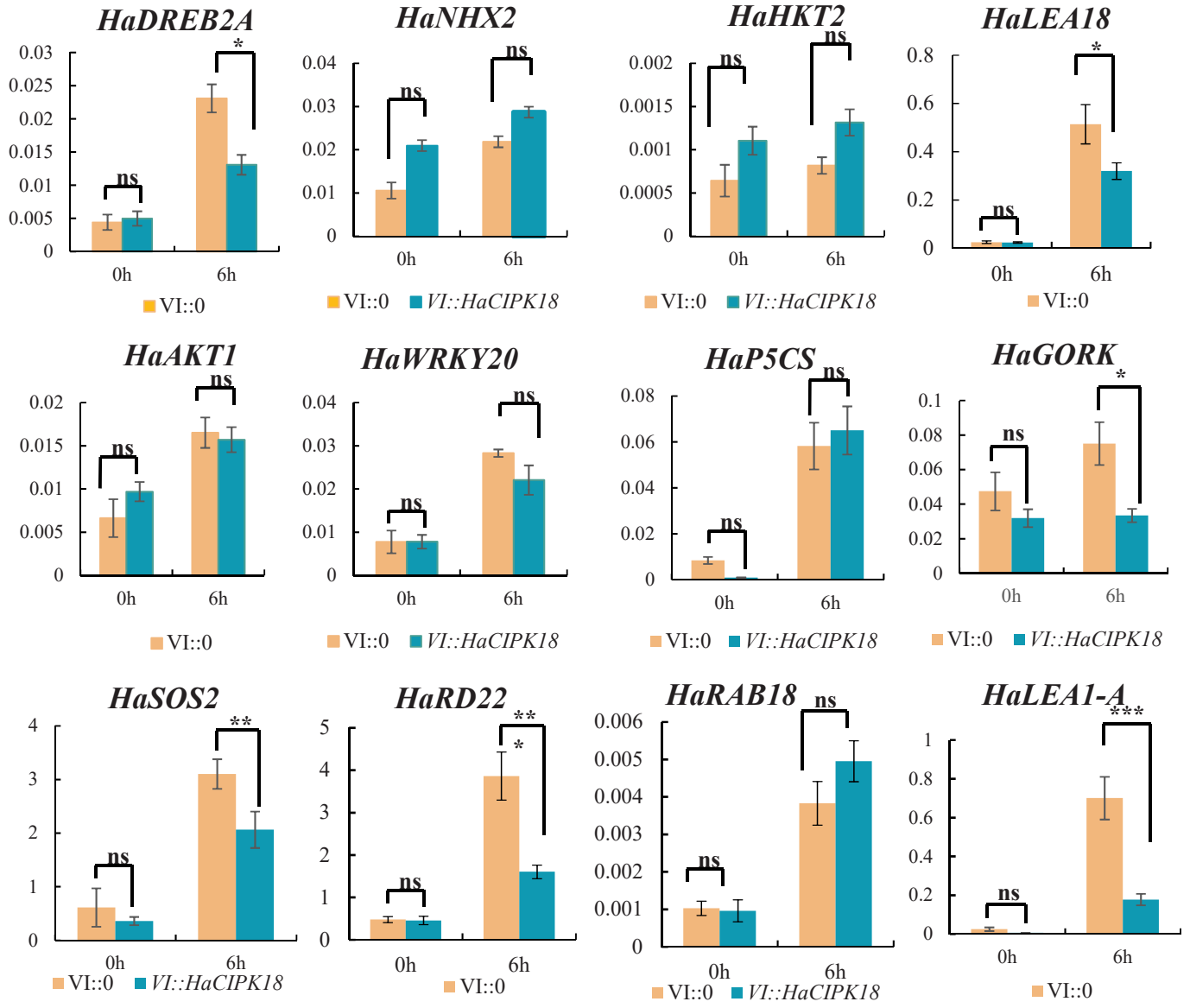

Fig. 9. Differential expression profiles of HaCIPK genes in response to NaCl treatment. Relative expression was quantified using the 2ˆ(-ΔΔCt) method with three replicates, normalised according to HaTubulin internal control. The values represent the mean and standard deviation obtained from three biological replicates. Asterisks indicate statistically significant comparisons with corresponding NaCl at 0 h (* $p < 0.05$, ** $p < 0.01$, *** $p < 0.001$).

Ca^{2+} signals to activate HaCIPK18, thereby enabling it to perform its phosphorylation function and regulate the downstream salt response network. This is similar to the mechanism by which the CIPK-CBL molecular module exercises its function in other plants. In *Arabidopsis*, CIPK24 (SOS2) is recruited by CBL4 (SOS3) and CBL5, which in turn activates SOS1 to form the SOS pathway to regulate ionic homeostasis in plant cells under salt stress, and CIPK8 is recruited by CBL10 to form a complex that also activates SOS1 in response to salt stress(Xie et al., 2024). In contrast, in rice, OsCIPK17 interacts with OsCBL2 and OsCBL3 and is the main module regulating Na^+ efflux from the aboveground in *Arabidopsis thaliana* during salt stress (Qin et al., 2024). However, the mechanism of how the HaCIPK18-HaCBL10 molecular module regulates the downstream salt-responsive genes is still unclear, and it is still necessary to resolve the mechanism of action of the HaCIPK18-HaCBL10 molecular module in response to salt stress by constructing VIGS-silenced lines of the *HaCBL10* gene and observing their phenotypes under salt stress.

At the level of salt stress response mechanism, salt response-related genes were identified at the transcriptional level in VIGS-mediated *HaCIPK18* gene-silenced lines, and it was confirmed that *HaCIPK18* was involved in salt stress by affecting the expression of six salt response-related genes, namely, *HaDREB2A, HaRD22, HaLEA18, HaLEA1-A, HaSOS2, HaGORK*(Fig. 9). A detailed analysis of these salt-responsive genes has revealed that *AtSOS2*, the homolog of *HaSOS2* in *Arabidopsis*, regulates the expression of SOS1 through co-regulation with SOS3. This, in turn, regulates Na^+ efflux from the cytoplasm during salt stress. Concurrently, the encoded protein has the capacity to bind physically to AtAFP2 protein, thereby forming a complex. This, in turn, results in the degradation of ABI5 protein, a negative transcription factor for seed germination under salt stress, thus contributing to the salt response process in plants. In contrast, in rice, the *HaGORK* homologous gene *OsGORK* encodes an outward shaker-type K^+ channel protein. This protein is involved in both the secretion of K^+ into the xylem sap and the control of stomatal aperture and leaf transpiration. It does this by driving the exocytosis of K^+ from the guard cells in order to close the stomata. This, in turn, improves plant salt tolerance(Zhou et al., 2022). Furthermore, *OsDREB2A*, the homologue of *HaDREB2A* in rice, is a member of the DREBP subfamily of AP2/ERF transcription factors. The

expression of *OsDREB2A* in soybean has been shown to enhance salt tolerance by increasing the accumulation of osmotic substances (e.g. soluble sugars and free proline) and by increasing the expression levels of some stress-responsive transcription factors and key genes (Zhang et al., 2013). HaCIPK18 integrates multiple salt tolerance pathways by regulating key genes like HaSOS2 and HaGORK, supporting its role as a core salt stress regulator in sunflower.

5. Conclusions

This study provides the first comprehensive genomic and functional characterization of the CIPK family in sunflower, identifying 36 *HaCIPK* genes and delineating their evolutionary characteristics. Through integrated bioinformatic and experimental approaches, we demonstrate that *HaCIPK18* serves as a key positive regulator of salt tolerance, a finding substantiated by its strong salt-induced expression, hypersensitivity phenotypes in VIGS-silenced lines, dysregulation of ROS homeostasis, and impaired induction of key salt-responsive effectors. Notably, *HaCIPK18* shows a developmentally specific expression pattern, with its expression shifting from roots during vegetative growth to floral styles at anthesis, raising the possibility that it may fulfill dual roles in stress adaptation and reproductive development. Using yeast two-hybrid and luciferase complementation imaging assays, we screened and identified HaCBL10 as an interacting partner of HaCIPK18; together, they form the HaCIPK18-HaCBL10 molecular module.

These results establish sunflower CIPKs as a conserved yet specialized signaling module, with *HaCIPK18* emerging as a critical node for salt stress resilience. Future work should clarify the precise molecular mechanisms underlying *HaCIPK18*'s dual functions and explore the broader roles of the HaCIPK family in abiotic stress adaptation in this agronomically significant crop.

CRediT authorship contribution statement

Qixiu Huang: Investigation, Data curation. **Maohong Cai:** Methodology. **Jiafeng Gu:** Investigation. **Liang Liang:** Writing – review & editing. **Zhonghua Lei:** Visualization. **Tao Chen:** Writing – review & editing, Funding acquisition. **Chenchang Wang:** Writing – original draft, Investigation.

Declaration of Competing Interest

All authors have read and complied with the journal's policies on competing interests. No authors have any financial or personal relationships with other people or organizations that could inappropriately influence or bias this work.

All authors declare that they have no competing interests to disclose.

Appendix A. Supporting information

Supplementary data associated with this article can be found in the online version at doi:10.1016/j.plantsci.2025.112846.

Data availability

Data will be made available on request.

References

Akram, U., Song, Y., Liang, C., Abid, M.A., Askari, M., Myat, A.A., et al., 2020. Genome-Wide Characterization and Expression Analysis of NHX Gene Family under Salinity Stress in Gossypium barbadense and Its Comparison with Gossypium hirsutum. Genes (Basel) 11.

Albrecht, V., Ritz, O., Linder, S., Harter, K., Kudla, J., 2001. The NAF domain defines a novel protein-protein interaction module conserved in Ca2+-regulated kinases. Embo J. 20, 1051–1063.

Aslam, M., Greaves, J.G., Jakada, B.H., Fakher, B., Wang, X., Qin, Y., 2022. AcCIPK5, a pineapple CBL-interacting protein kinase, confers salt, osmotic and cold stress tolerance in transgenic Arabidopsis. Plant Sci. 320, 111284.

Chen, X., Chen, G., Li, J., Hao, X., Tuerxun, Z., Chang, X., et al., 2021a. A maize calcineurin B-like interacting protein kinase ZmCIPK42 confers salt stress tolerance. Physiol. Plant 171, 161–172.

Chen, X., Ding, Y., Yang, Y., Song, C., Wang, B., Yang, S., et al., 2021b. Protein kinases in plant responses to drought, salt, and cold stress. J. Integr. Plant Biol. 63, 53–78.

Di, T., Wu, Y., Feng, X., He, M., Lei, L., Wang, J., et al., 2024. CIPK11 phosphorylates GSTU23 to promote cold tolerance in Camellia sinensis. Plant Cell Environ. 47, 4786–4799.

Gong, D., Guo, Y., Schumaker, K.S., Zhu, J.K., 2004. The SOS3 family of calcium sensors and SOS2 family of protein kinases in Arabidopsis. Plant Physiol. 134, 919–926.

Hashimoto, K., Kudla, J., 2011. Calcium decoding mechanisms in plants. Biochimie 93, 2054–2059.

He, L., Yang, X., Wang, L., Zhu, L., Zhou, T., Deng, J., et al., 2013. Molecular cloning and functional characterization of a novel cotton CBL-interacting protein kinase gene (GhCIPK6) reveals its involvement in multiple abiotic stress tolerance in transgenic plants. Biochem Biophys. Res Commun. 435, 209–215.

Imtiaz, K., Ahmed, M., Annum, N., Tester, M., Saeed, N.A., 2023. AtCIPK16, a CBL-interacting protein kinase gene, confers salinity tolerance in transgenic wheat. Front Plant Sci. 14, 1127311.

Jiao, F., Zhang, D., Chen, Y., Wu, J., 2024. Genome-Wide Identification of Members of the Soybean CBL Gene Family and Characterization of the Functional Role of GmCBL1 in Responses to Saline and Alkaline Stress. Plants (Basel) 13.

Kaya, C., Uğurlar, F., Adamakis, I.S., 2024. Molecular Mechanisms of CBL-CIPK Signaling Pathway in Plant Abiotic Stress Tolerance and Hormone Crosstalk. Int J. Mol. Sci. 25.

Khan, F.S., Goher, F., Paulsmeyer, M.N., Hu, C.G., Zhang, J.Z., 2023. Calcium (Ca(2+)) sensors and MYC2 are crucial players during jasmonates-mediated abiotic stress tolerance in plants. Plant Biol. (Stuttg.) 25, 1025–1034.

Kim, B.G., Waadt, R., Cheong, Y.H., Pandey, G.K., Dominguez-Solis, J.R., Schültke, S., et al., 2007. The calcium sensor CBL10 mediates salt tolerance by regulating ion homeostasis in Arabidopsis. Plant J. 52, 473–484.

Kollist, H., Zandalinas, S.I., Sengupta, S., Nuhkat, M., Kangasjärvi, J., Mittler, R., 2019. Rapid Responses to Abiotic Stress: Priming the Landscape for the Signal Transduction Network. Trends Plant Sci. 24, 25–37.

Kolukisaoglu, U., Weinl, S., Blazevic, D., Batistic, O., Kudla, J. r, 2004. Calcium sensors and their interacting protein kinases: genomics of the Arabidopsis and rice CBL-CIPK signaling networks. Plant Physiol. 134, 43–58.

Kopecká, R., Kameniarová, M., Černý, M., Brzobohatý, B., Novák, J., 2023. Abiotic stress in crop production. Int. J. Mol. Sci. 24, 6603.

Kour, J., Khanna, K., Singh, A.D., Dhiman, S., Bhardwaj, T., Devi, K., et al., 2023. Calcium's multifaceted functions: From nutrient to secondary messenger during stress. South Afr. J. Bot. 152, 247–263.

Kudla, J., Batistic, O., Hashimoto, K., 2010. Calcium signals: the lead currency of plant information processing. Plant Cell 22, 541–563.

Li, K.L., Tang, R.J., Wang, C., Luan, S., 2023. Potassium nutrient status drives posttranslational regulation of a low-K response network in Arabidopsis. Nat. Commun. 14, 360.

Li, R., Zhang, J., Wei, J., Wang, H., Wang, Y., Ma, R., 2009. Functions and mechanisms of the CBL–CIPK signaling system in plant response to abiotic stress. Prog. Nat. Sci. 19, 667–676.

Liu, J., Ishitani, M., Halfter, U., Kim, C.S., Zhu, J.K., 2000. The Arabidopsis thaliana SOS2 gene encodes a protein kinase that is required for salt tolerance. Proc. Natl. Acad. Sci. USA 97, 3730–3734.

Luan, S., Kudla, J., Rodriguez-Concepcion, M., Yalovsky, S., Gruissem, W., 2002. Calmodulins and calcineurin B-like proteins: calcium sensors for specific signal response coupling in plants. Plant Cell 14, S389–S400.

Ma, X., Gai, W.X., Li, Y., Yu, Y.N., Ali, M., Gong, Z.H., 2022. The CBL-interacting protein kinase CaCIPK13 positively regulates defence mechanisms against cold stress in pepper. J. Exp. Bot. 73, 1655–1667.

Ma, X., Li, Q.H., Yu, Y.N., Qiao, Y.M., Haq, S.U., Gong, Z.H., 2020. The CBL-CIPK Pathway in Plant Response to Stress Signals. Int J. Mol. Sci. 21.

Mao, J., Manik, S.M., Shi, S., Chao, J., Jin, Y., Wang, Q., et al., 2016. Mechanisms and Physiological Roles of the CBL-CIPK Networking System in Arabidopsis thaliana. Genes (Basel) 7.

Martínez-Martínez, A., Amo, J., Jiménez-Estévez, E., Lara, A., Martínez, V., Rubio, F., et al., 2024. SlCIPK9 regulates pollen tube elongation in tomato plants via a K(+)-independent mechanism. Plant Physiol. Biochem 215, 109039.

Moroldo, M., Blanchet, N., Duruflé, H., Bernillon, S., Berton, T., Fernandez, O., et al., 2024. Genetic control of abiotic stress-related specialized metabolites in sunflower. BMC Genom. 25, 199.

Patra, N., Hariharan, S., Gain, H., Maiti, M.K., Das, A., Banerjee, J., 2021. TypiCal but DeliCate Ca(++)re: Dissecting the Essence of Calcium Signaling Network as a Robust Response Coordinator of Versatile Abiotic and Biotic Stimuli in Plants. Front Plant Sci. 12, 752246.

Qin, X., Zhang, X., Ma, C., Yang, X., Hu, Y., Liu, Y., et al., 2024. Rice OsCIPK17-OsCBL2/3 module enhances shoot Na(+) exclusion and plant salt tolerance in transgenic Arabidopsis. Plant Physiol. Biochem 215, 109034.

Shi, D., Sheng, Y., 2005. Effect of various salt–alkaline mixed stress conditions on sunflower seedlings and analysis of their stress factors. Environ. Exp. Bot. 54, 8–21.

Smith, B.D., 2014. The domestication of Helianthus annuus L. (sunflower). Veg. Hist. Archaeobotany 23, 57–74.

Tian, F., Chang, E., Li, Y., Sun, P., Hu, J., Zhang, J., 2017. Expression and integrated network analyses revealed functional divergence of NHX-type Na(+)/H(+) exchanger genes in poplar. Sci. Rep. 7, 2607.

Wang, C., Tang, R.J., Kou, S., Xu, X., Lu, Y., Rauscher, K., et al., 2024. Mechanisms of calcium homeostasis orchestrate plant growth and immunity. Nature 627, 382–388.
Wu, Y., Luo, Q., Wu, Z., Yu, J., Zhang, Q., Shi, F., et al., 2023. A straight-forward gene mining strategy to identify TaCIPK19 as a new regulator of drought tolerance in wheat. Plant Physiol. Biochem 203, 108034.
Xiao, C., Zhang, H., Xie, F., Pan, Z.Y., Qiu, W.M., Tong, Z., et al., 2022. Evolution, gene expression, and protein-protein interaction analyses identify candidate CBL-CIPK signalling networks implicated in stress responses to cold and bacterial infection in citrus. BMC Plant Biol. 22, 420.
Xie, Q., Yin, X., Wang, Y., Qi, Y., Pan, C., Sulaymanov, S., et al., 2024. The signalling pathways, calcineurin B-like protein 5 (CBL5)-CBL-interacting protein kinase 8 (CIPK8)/CIPK24-salt overly sensitive 1 (SOS1), transduce salt signals in seed germination in Arabidopsis. Plant Cell Environ. 47, 1486–1502.
Yang, L., Zhang, N., Wang, K., Zheng, Z., Wei, J., Si, H., 2023. CBL-Interacting Protein Kinases 18 (CIPK18) Gene Positively Regulates Drought Resistance in Potato. Int J. Mol. Sci. 24.
Yang, W., Kong, Z., Omo-Ikerodah, E., Xu, W., Li, Q., Xue, Y., 2008. Calcineurin B-like interacting protein kinase OsCIPK23 functions in pollination and drought stress responses in rice (Oryza sativa L.). J. Genet. Genom. 35, 531–S532.
Yang, Y., Guo, Y., 2018. Elucidating the molecular mechanisms mediating plant salt-stress responses. N. Phytol. 217, 523–539.
Yin, X., Xia, Y., Xie, Q., Cao, Y., Wang, Z., Hao, G., et al., 2020. The protein kinase complex CBL10-CIPK8-SOS1 functions in Arabidopsis to regulate salt tolerance. J. Exp. Bot. 71, 1801–1814.
Zhang, H., Yang, B., Liu, W.Z., Li, H., Wang, L., Wang, B., et al., 2014. Identification and characterization of CBL and CIPK gene families in canola (Brassica napus L.). BMC Plant Biol. 14, 8.
Zhang, T., Li, Y., Wang, P., Luo, Q., Fu, S., Kang, Y., et al., 2023. Characterization of Dendrobium catenatum CBL-CIPK signaling networks and their response to abiotic stress. Int J. Biol. Macromol. 236, 124010.
Zhang, X.X., Tang, Y.J., Ma, Q.B., Yang, C.Y., Mu, Y.H., Suo, H.C., et al., 2013. OsDREB2A, a rice transcription factor, significantly affects salt tolerance in transgenic soybean. PLoS One 8, e83011.
Zhang, Y., Zhou, X., Liu, S., Yu, A., Yang, C., Chen, X., et al., 2019. Identification and Functional Analysis of Tomato CIPK Gene Family. Int J. Mol. Sci. 21.
Zhou, J., Nguyen, T.H., Hmidi, D., Luu, D.T., Sentenac, H., Véry, A.A., 2022. The outward shaker channel OsK5.2 improves plant salt tolerance by contributing to control of both leaf transpiration and K(+) secretion into xylem sap. Plant Cell Environ. 45, 1734–1748.
Zhou, Z., Tang, W., Sun, Z., Li, J., Yang, B., Liu, Y., et al., 2023. OsCIPK9 Interacts with OsSOS3 and Affects Salt-Related Transport to Improve Salt Tolerance. Plants (Basel) 12.
Zhu, K., Chen, F., Liu, J., Chen, X., Hewezi, T., Cheng, Z.M., 2016. Evolution of an intron-poor cluster of the CIPK gene family and expression in response to drought stress in soybean. Sci. Rep. 6, 28225.